Journal of proteome research

pubs.acs.org/jpr

Article

Exploring Infantile Epileptic Spasm Syndrome: A Proteomic Analysis of Plasma Using the Data-Independent Acquisition Approach

Haohua Huang, Dezhi Cao, Yan Hu, Qianqian He, Xia Zhao, Li Chen, Sufang Lin, Xufeng Luo, Yuanzhen Ye, Jianxiang Liao, Huafang Zou, and Dongfang Zou*

Cite This: J. Proteome Res. 2024, 23, 4316−4326

Read Online

ACCESS | Metrics & More | Article Recommendations | Supporting Information

ABSTRACT: This study aimed to identify characteristic proteins in infantile epileptic spasm syndrome (IESS) patients' plasma, offering insights into potential early diagnostic biomarkers and its underlying causes. Plasma samples were gathered from 60 patients with IESS and 40 healthy controls. Data-independent acquisition proteomic analysis was utilized to identify differentially expressed proteins (DEPs). These DEPs underwent functional annotation through Gene Ontology (GO) and the Kyoto Encyclopedia of Genes and Genomes (KEGG) pathway enrichment analyses. Gene set enrichment analysis (GSEA) was employed for both GO (GSEA-GO) and KEGG (GSEA-KEGG) analyses to examine the gene expression profiles. Receiver operating characteristic (ROC) curves assessed biomarkers' discriminatory capacity. A total of 124 DEPs were identified in IESS patients' plasma, mainly linked to pathways, encompassing chemokines, cytokines, and oxidative detoxification. GSEA-GO and GSEA-KEGG analyses indicated significant enrichment of genes associated with cell migration, focal adhesion, and phagosome pathways. ROC curve analysis demonstrated that the combination of PRSS1 and ACTB, PRSS3, ACTB, and PRSS1 alone exhibited AUC values exceeding 0.7. This study elucidated the significant contribution of cytokines, chemokines, oxidative detoxification, and phagosomes to the IESS pathogenesis. The combination of PRSS1 and ACTB holds promise as biomarkers for the early diagnosis of IESS.

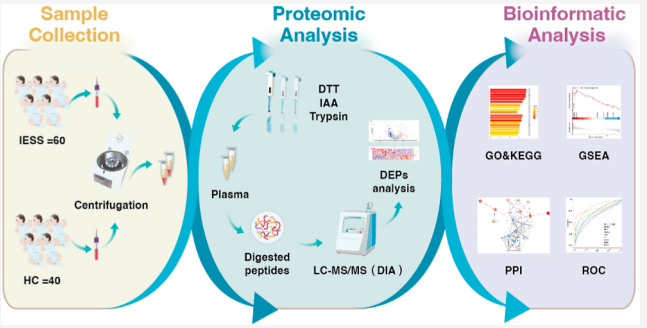

KEYWORDS: *infantile epileptic spasm syndrome, biomarker, data-independent acquisition, plasma*

INTRODUCTION

Infantile epileptic spasm syndrome (IESS) has been reclassified by the latest International League Against Epilepsy (ILAE) classification in 2022 to encompass patients who may not fully meet the criteria of West syndrome.[1] The mandatory diagnostic criteria for West syndrome include epileptic spasms, interictal electroencephalography (EEG) demonstrating hypsarrhythmia, and developmental delay or regression. This encephalopathy primarily affects infants and young children before the age of 2 years, with a characteristic of strict age dependence during early infancy.[2] The incidence of this condition varies between 2 and 5 per 10,000 successful live births.[3] In children diagnosed with IESS, persistent epileptic activity can lead to progressive cognitive and behavioral impairments,[4,5] significantly affecting their long-term quality of family life.[6] However, intellectual disability remains a common outcome among IESS patients, persisting even after the cessation of spasms and hypsarrhythmia. The molecular mechanisms underlying the disorder and its prognosis remain elusive.

Recent advancements in high-throughput proteomics methodologies, such as data-independent acquisition (DIA), have facilitated extensive profiling of blood proteomics on a large scale. These technologies have been widely utilized in the study of central nervous system diseases including epilepsy. As a result, they led to the identification of novel biomarkers and provided valuable biological annotations for understanding disease mechanisms.[7,8] There is a scarcity of DIA-mass spectrometry (DIA-MS) studies concentrating on the plasma proteome analysis of children with IESS. Hence, this study employed the DIA proteomics technology to explore and assess differentially expressed proteins (DEPs) in IESS patients compared with healthy controls, aiming to unravel the protein regulatory network associated with IESS. The ultimate objective was to investigate the protein-level pathogenesis of IESS and discover biomarkers crucial for diagnosing and predicting the disease.

Received: April 11, 2024
Revised: May 23, 2024
Accepted: May 24, 2024
Published: June 10, 2024

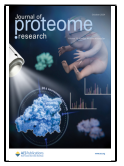

https://doi.org/10.1021/acs.jproteome.4c00298
J. Proteome Res. 2024, 23, 4316−4326

Table 1. Demographics Data and Clinical Characteristics of IESS Patients and Age-and-Gender Matched Healthy Controls

	IESS patients; *n* (%)	healthy controls; n (%)
	Gender	
male	33 (55.0)	20 (50.0)
female	27 (44.0)	20 (50.0)
	Age (Month)	
mean ± SD	8.8 ± 4.9	12.0 ± 4.0
min−max	0.6−25.0	3.0−23.0
	Age of Onset (Month)	
mean ± SD	5.5 ± 3.7	−
min−max	0−17	−
	Developmental Delay	
yes	37 (61.7)	
no	23 (38.3)	
	Other Systemic Malformations	
yes	23 (38.3)	−
no	37 (61.7)	−
	Abnormal Genetic Results	
yes	19 (31.7)	−
no	25 (41.7)	−
without genetic results	16 (26.6)	−
	Abnormal Neurological Examination	
yes	42 (70.0)	−
no	18 (30.0)	−
	Abnormal MRI	
yes	25 (41.7)	−
no	35 (58.3)	−

EXPERIMENTAL SECTION

Participants' Recruitment and Eligibility Criteria

A total of 60 patients with IESS and 40 healthy controls were recruited from the Department of Neurology and Children's Health Care of Shenzhen Children's Hospital (Shenzhen, China) between October 2020 and December 2022. This study received the approval from the Ethics Committee of the Shenzhen Children's Hospital (Approval no. 202200802). Each patient's parents or legal guardians provided written informed consent. Clinical evaluations were conducted by pediatric neurologists, and diagnosis was made based on seizure type, electroencephalographic findings, and brain imaging results. Inclusion criteria comprised age <2 years and diagnosis of IESS according to the ILAE criteria (2022).[1] Exclusion criteria included patients with seizures likely caused by acquired brain injuries, such as head trauma, brain tumors, and CNS infections; those who had received allogeneic blood product transfusion over the past 2 months; and those with hemolytic disease. Healthy controls, who were less than 2 years old, had no personal or family history of epilepsy. All of the recruited children were of Chinese ethnicity.

Preparation of Proteins

A venous blood sample of 5 mL was collected into an EDTA blood collection tube and gently mixed by inverting the tube 5−10 times. The samples were then allowed to stand for 30 min (to prevent hemolysis, avoiding violent shaking). Afterward, the samples were centrifuged at 2000*g* for 10 min at 4 °C using a swinging bucket rotor. The supernatants were carefully collected, aliquoted, frozen in liquid nitrogen, and then stored at −80 °C until use. Before utilization, the stored plasma was thawed in water for 5−10 min. To prepare the samples for analysis, the supernatants were supplemented with sample desalting and treatment (SDT) buffer (4% sodium dodecyl sulfate, 1 nM dithiothreitol (DTT), 100 mM Tris−HCl, pH 7.6) and subjected to a 15 min boil. Following centrifugation at 14,000*g* for 20 min, the supernatants were quantified using the BCA protein assay kit (Bio-Rad, Hercules, CA, USA). Each sample was then supplemented with DTT to reach a final concentration of 40 mM and mixed at 600 rpm for 1.5 h at 37 °C. Postcooling to room temperature, IAA was added with a final concentration of 20 mM to block reduced cysteine residues, and the samples were then left to incubate in darkness for 30 min. The subsequent steps involved transferring the samples to Microcon units (10 kDa) and thrice washing with 100 μL of UA buffer, followed by twice rinsing with 100 μL of 25 mM NH_4HCO_3 buffer.

Next, trypsin was introduced to each sample at a trypsin-to-protein (w/w) ratio of 1:50, and the samples were incubated at 37 °C for 15−18 h (overnight). The resulting peptides were collected as a filtrate. Following this, the peptides from each sample underwent desalting using C18 Cartridges [Empore SPE Cartridges C18 (standard density), bed I.D. 7 mm, volume 3 mL; Sigma-Aldrich, MO, USA], concentrated via vacuum centrifugation, and dissolved in 40 μL of 0.1% (v/v) formic acid. The peptide concentration was determined by measuring the UV absorbance at 280 nm. Indexed retention time (IRT) calibration peptides were added to the samples for DIA experiments. The digested pool peptides underwent fractionation into 10 fractions using a Thermo Scientific Pierce High pH Reversed-Phase Peptide Fractionation kit, with only low-abundance components fractionated for serum/plasma samples. Each fraction was desalted utilizing C18 Cartridges and reconstituted in 40 μL of 0.1% (v/v) formic acid. Prior to data-dependent acquisition (DDA) analysis, the samples were spiked with iRT-Kits peptides from Biognosys (Schlieren, Switzerland).

https://doi.org/10.1021/acs.jproteome.4c00298
J. Proteome Res. 2024, 23, 4316−4326

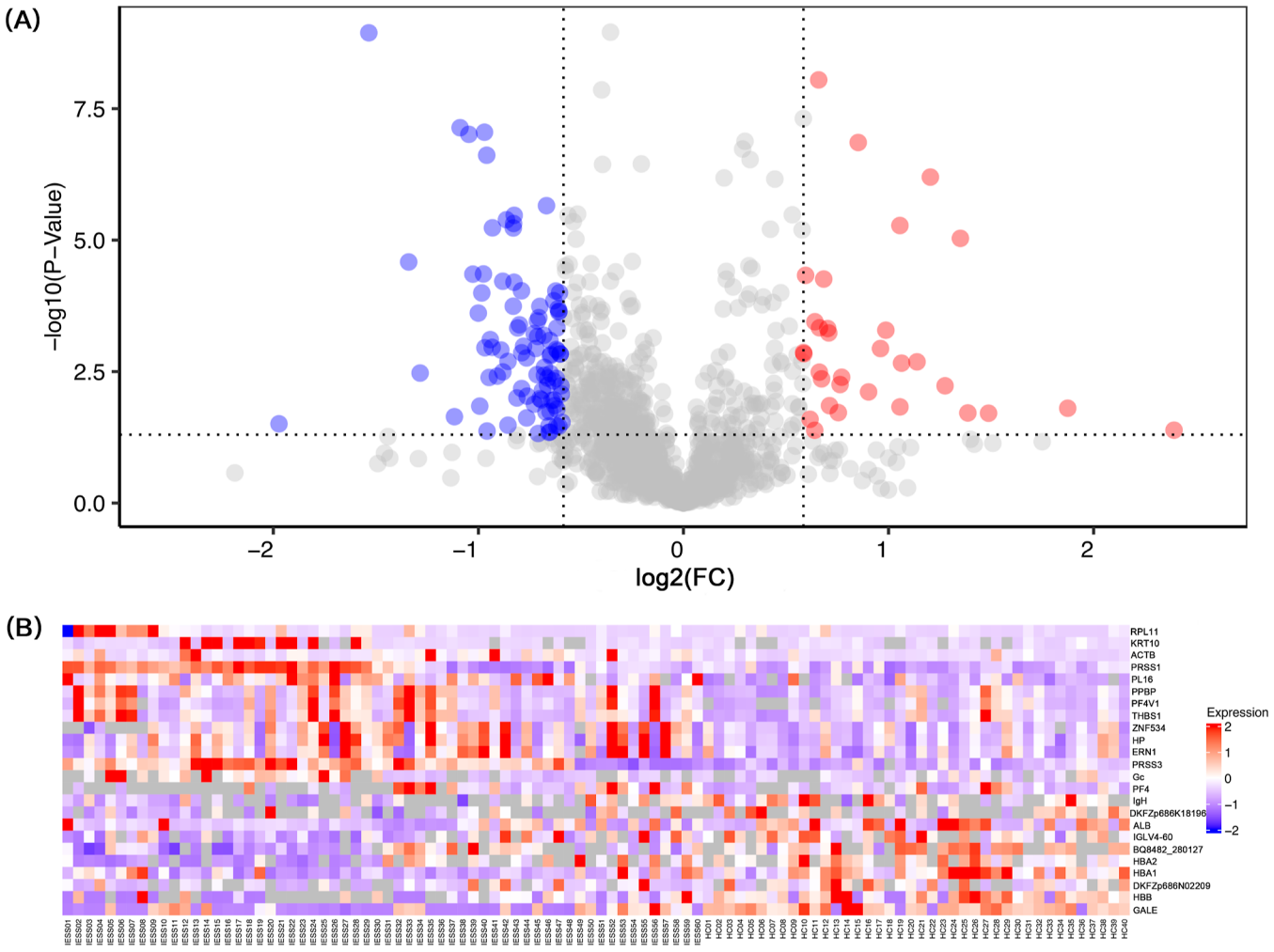

Figure 1. DEPs in plasma of patients with IESS and healthy controls. (A) Volcano plot illustrating DEPs. (B) Heat map illustrating the cluster analysis of DEPs. Red indicates significant upregulation, while blue indicates significant downregulation.

Liquid Chromatography-Tandem Mass Spectrometry (LC−MS/MS)

The chromatographic separation was conducted using a liquid chromatograph (Easy-nLC 1200, Thermo Scientific). A C18 analytical column (Thermo Scientific, ES802, 1.9 μm, 75 μm × 20 cm) was utilized for linear gradient separation, employing buffer B consisting of 84% acetonitrile and 0.1% formic acid at a flow rate of 300 nL/min. The MS-SIM full-range scan was set from 350 to 1800 m/z with a resolution of 60,000. Subsequently, 20 ddMS2 scans were performed according to the provided table using an isolation window of 1.5 m/z and a resolution of 30,000 ($@m/z200$). The ddMS2 scans were carried out in the DIA data acquisition mode, utilizing 44 DIA acquisition windows.

MS Data Analysis and DEP Identification

DEPs were identified through the construction of a library using the DDA method and subsequent qualitative and quantitative analyses using the DIA model. Spectronaut 14.4.200727.47784 (Biognosys) software was employed for data retrieval and DIA data analysis. All reported data met a stringent criterion of 99% confidence for protein identification, determined by a false discovery rate ≤ 1%. The fold change (FC) between IESS patients and healthy controls was calculated as the average expression rate. DEPs were screened based on criteria of logFC > 1.5 or logFC < 0.67, with a level of significance set at $P < 0.05$.

Gene Ontology (GO) and Kyoto Encyclopedia of Genes and Genomes (KEGG) Pathway Enrichment Analyses

To identify significant pathways, the GO and KEEG pathway enrichment analyses were conducted using the clusterProfiler package (version 4.10.0). The GO enrichment analysis included the assessment of the biological process (BP), cellular component (CC), and molecular function (MF). The GO and KEEG pathway enrichment analyses were executed with the Benjamini-Hochberg method to mitigate the bias. A significance threshold of $P < 0.05$ was also applied.

Gene Set Enrichment Analysis-Based GO (GSEA-GO) and GSEA-Based KEGG (GSEA-KEGG) Pathway Analyses

GSEA, a computational approach for genome-wide expression profile microarray data analysis, was performed by using the clusterProfiler package (version 4.10.0). The alteration in gene expression between IESS patients and healthy controls was calculated, and a gene list was generated based on the absolute value of the logarithm of the fold change (|log2FC|). GO analysis and KEGG pathway enrichment analyses were performed by using gseGO and gseKEGG functions, respectively, through the clusterProfiler package. A significant threshold of $P < 0.05$ was established as the cutoff criterion.

https://doi.org/10.1021/acs.jproteome.4c00298
J. Proteome Res. 2024, 23, 4316−4326

Table 2. 24 Most Significantly Differentially Expressed Proteins (DEPs)

protein	gene symbol	protein descriptions	fold-change	P	style
P62913	RPL11	60S ribosomal protein L11	3.66	1.57×10^{-2}	up
P13645	KRT10	keratin, type I cytoskeletal 10	2.80	1.95×10^{-2}	up
P60709	ACTB	actin, cytoplasmic 1	2.61	1.93×10^{-2}	up
E7EQ64	PRSS1	trypsin-1	2.30	6.32×10^{-7}	up
Q6UXB8	PI16	peptidase inhibitor 16	2.08	5.27×10^{-6}	up
P02775	PPBP	platelet basic protein	1.98	5.16×10^{-4}	up
P10720	PF4V1	platelet factor 4 variant	1.87	7.70×10^{-3}	up
A0A024R9Q1	THBS1	thrombospondin 1, isoform CRA a	1.70	5.57×10^{-3}	up
Q76KX8	ZNF534	zinc finger protein 534	1.63	5.81×10^{-4}	up
P00738	HP	haptoglobin	1.63	4.80×10^{-4}	up
O75460	ERN1	serine/threonine-protein kinase/endoribonuclease IRE1	1.58	3.24×10^{-3}	up
A1A508	PRSS3	PRSS3 protein	1.58	8.97×10^{-9}	up
A0A1B1CYC5	Gc	vitamin D binding protein (fragment)	1.56	4.12×10^{-2}	up
P02776	PF4	platelet factor 4	1.53	2.55×10^{-2}	up
A0A2U8J8Q0	IgH	Ig heavy chain variable region (fragment)	0.66	1.46×10^{-3}	down
Q6N092	DKFZp686 K18196	uncharacterized protein DKFZp686 K18196 (fragment)	0.64	1.12×10^{-2}	down
A0A075B6I1	IGLV4−60	immunoglobulin lambda variable 4−60	0.63	4.21×10^{-3}	down
A0A087WWT3	ALB	plasma albumin	0.64	3.44×10^{-3}	down
A0A2P9AMP2	BQ8482_280127	uncharacterized protein	0.63	2.21×10^{-6}	down
Q96T46	HBA2	hemoglobin alpha 2 (fragment)	0.57	4.07×10^{-4}	down
Q86YQ4	HBA1	alpha-1 globin (fragment)	0.56	4.83×10^{-6}	down
P68223	HBB	hemoglobin subunit beta	0.50	2.44×10^{-4}	down
Q7Z351	DKFZp686N02209	uncharacterized protein DKFZp686N02209	0.50	1.43×10^{-2}	down
A0A024RAB7	GALE	UDP-galactose-4-epimerase, isoform CRA b	0.47	7.28×10^{-8}	down

Protein−Protein Interaction (PPI) Network

The STRING database (version 12.0, http://string-db.org/)[9] was utilized to retrieve the PPI network among the DEPs (Accession Date: March 15, 2024). The confidence score of the PPI was 0.4. In total, 24 proteins were selected based on the criteria of logFC > 1.5 or logFC < 0.67, with a significance threshold of $P < 0.05$, for inclusion in the PPI network analysis. The visualization and analysis of PPI networks of DEPs were conducted using R package ggraph (version 2.1.0) and igraph (version 1.5.1). The maximum number of interactions for each protein was limited to 5.

Receiver Operating Characteristic (ROC) Curves

The plot.roc() function in the pROC R package (version 1.18.5) was employed to plot the ROC curves. The discriminatory power of the candidate biomarkers was assessed by calculating the areas under the curve (AUCs) using the auc() function in the same package. The ROC curve analysis was carried out utilizing SPSS 22.0 software (IBM, Armonk, NY, USA).

Statistical Analysis and Data Visualization

The clusterProfiler R package (version 4.10.0) was utilized to screen the DEPs. DEPs were selected based on criteria, including logFC greater than 1.5 or less than 0.67, with a corresponding $P < 0.05$ determined by either Student's t-test or analysis of variance (ANOVA). A significance level of $P < 0.05$ was regarded as statistically significant. For data visualization, ComplexHeatmap (version 2.18.0) was employed to generate a heatmap of the DEPs. Additionally, a volcano plot was drawn using ggplot2 (version 3.4.4).

RESULTS

Demographics and Clinical Characteristics

A total of 60 IESS patients were enrolled, comprising 33 male patients and 27 female patients. Patients' ages spanned from 19 days to 25 months, with a mean age of 8.8 months. The age at seizure onset ranged from 1 day to 17 months, with a mean age of 5.5 months. Additionally, this study enrolled 40 healthy controls who matched the age and gender. Demographic and clinical data are summarized in Table 1.

Identification of DEPs

Using DIA-MS, 1487 shared proteins were identified across all patients' plasma samples. Principal component analysis (PCA) demonstrated a clear separation between IESS patients and healthy controls, highlighting the diagnostic accuracy of the samples (Figure S1). A Venn diagram displayed that 142 proteins were exclusive to IESS patients, while 71 proteins were exclusive to healthy controls (Figure S2). In total, 124 DEPs were detected in IESS patients' plasma samples compared with healthy controls, including 92 upregulated proteins and 32 downregulated proteins (Table S1). A volcano map was used to visualize the upregulated and downregulated DEPs (Figure 1.A). Table 2 summarizes the most significantly enriched DEPs, comprising 14 upregulated and 10 downregulated proteins. Furthermore, a hierarchical clustering heat map highlighted variations in protein expression patterns between IESS patients and healthy controls (Figure 1.B).

GO and KEGG Pathway Enrichment Analyses

To elucidate the biological roles of the DEPs, GO and KEGG pathway enrichment analyses were performed on the most significantly enriched DEPs, which were predicted to be associated with disease mechanisms. The GO enrichment analysis revealed that the DEPs in both groups were predominantly enriched in cellular oxidant detoxification, leukocyte chemotaxis, and response to chemokine in the BP category. In terms of CC, enrichment was found in the vesicle lumen and blood microparticle. In the MF category, enrichment was noted in chemokine receptor binding, cytokine receptor binding, haptoglobin binding, and sulfur compound binding

https://doi.org/10.1021/acs.jproteome.4c00298
J. Proteome Res. 2024, 23, 4316−4326

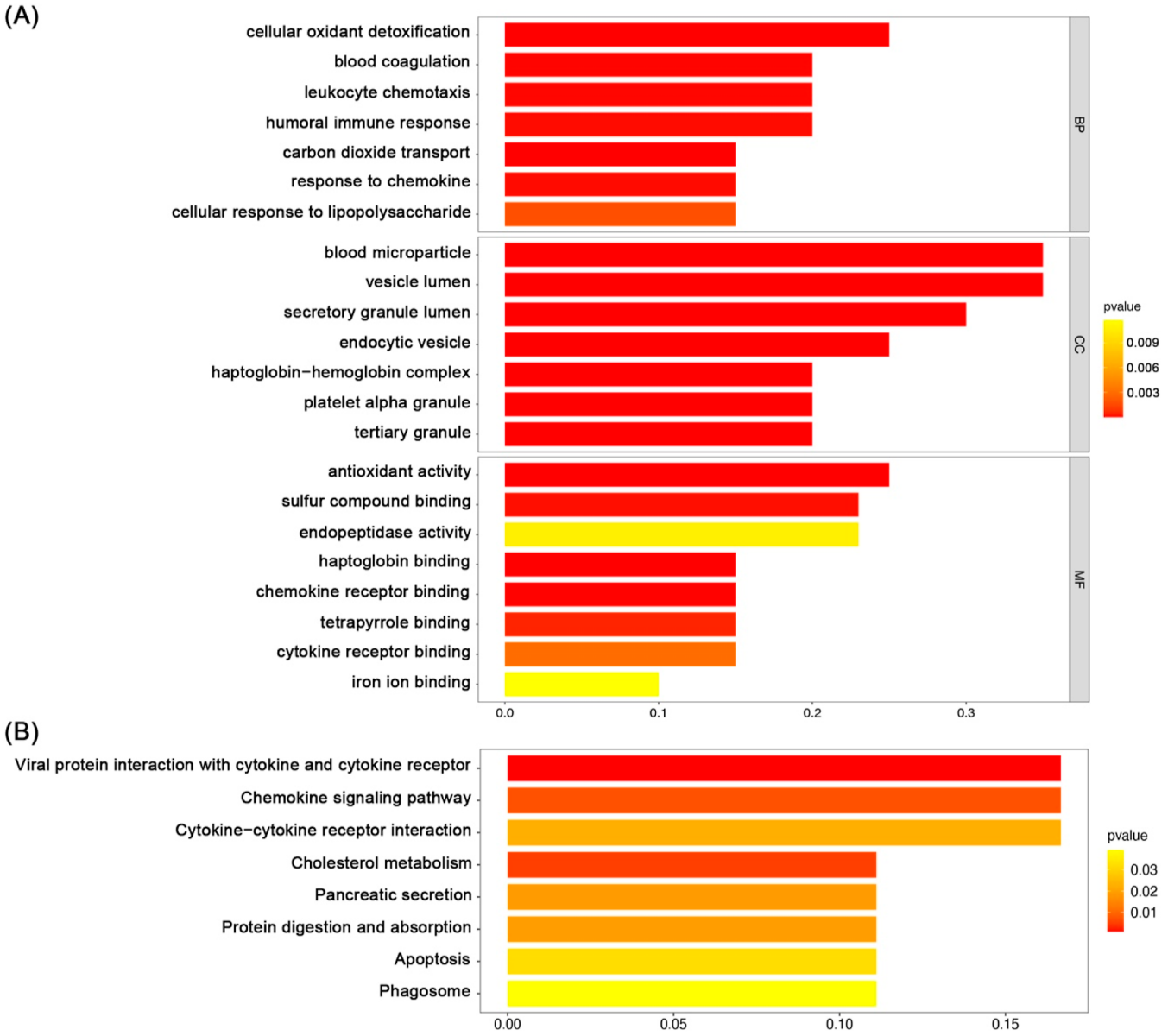

Figure 2. GO and KEGG pathway analyses of the most significantly enriched DEPs in IESS patients compared with healthy controls. (A) GO enrichment analysis included BP, CC, and MF categories. (B) KEGG pathway analysis. Each pathway was ranked by GeneRatio.

(Figure 2A). Furthermore, the KEGG pathway analysis revealed that the DEPs were primarily enriched in pathways linked to the cytokine−cytokine receptor interaction, the chemokine signaling pathway, and phagosomes between the two groups (Figure 2B). Further details regarding the outcomes of the GO and KEGG pathway enrichment analyses are presented in Tables S2 and S3, respectively.

GSEA

The GSEA was employed to identify the most significantly enriched GSEA-GO terms that were predicted to be associated with disease mechanisms among the BPs of GO. The enriched GSEA-GO terms are depicted in Figure 3A. Pathways enriched in cellular response to oxygen-containing compounds and cell migration were identified in BP. In CC, pathways enriched in the vesicle and nuclear lumen were noted. Lastly, in MF, pathways enriched in protein binding, sulfur compound binding, and endopeptidase activity were found. By employing GSEA to identify KEGG pathways relevant to IESS samples, it was revealed that the majority of these genes exhibited enrichment in focal adhesion, phagosomes, the PI3K-Akt signaling pathway, ECM-receptor interaction, and actin cytoskeleton regulation (Figure 3B). GSEA enrichment plots of representative gene sets on "phagosome" and "PI3K-Akt signaling pathway" are illustrated in Figure 3C,D, respectively. Further details regarding GSEA-GO and GSEA-KEEG are presented in Tables S4 and S5, respectively.

Identification of Hub Proteins by the PPI Network

To comprehensively investigate the molecular mechanism of IESS, a PPI network analysis was conducted to elucidate the relationship between proteins. A total of 124 DEPs were imported into STRING 12.0 software to generate the PPI network (Figure 4). The results revealed that ACTB, PF4V1, THBS1, HP, PF4, and PPBP served as hub proteins in the PPI network, suggesting strong associations of these proteins with the etiology of IESS.

https://doi.org/10.1021/acs.jproteome.4c00298
J. Proteome Res. 2024, 23, 4316−4326

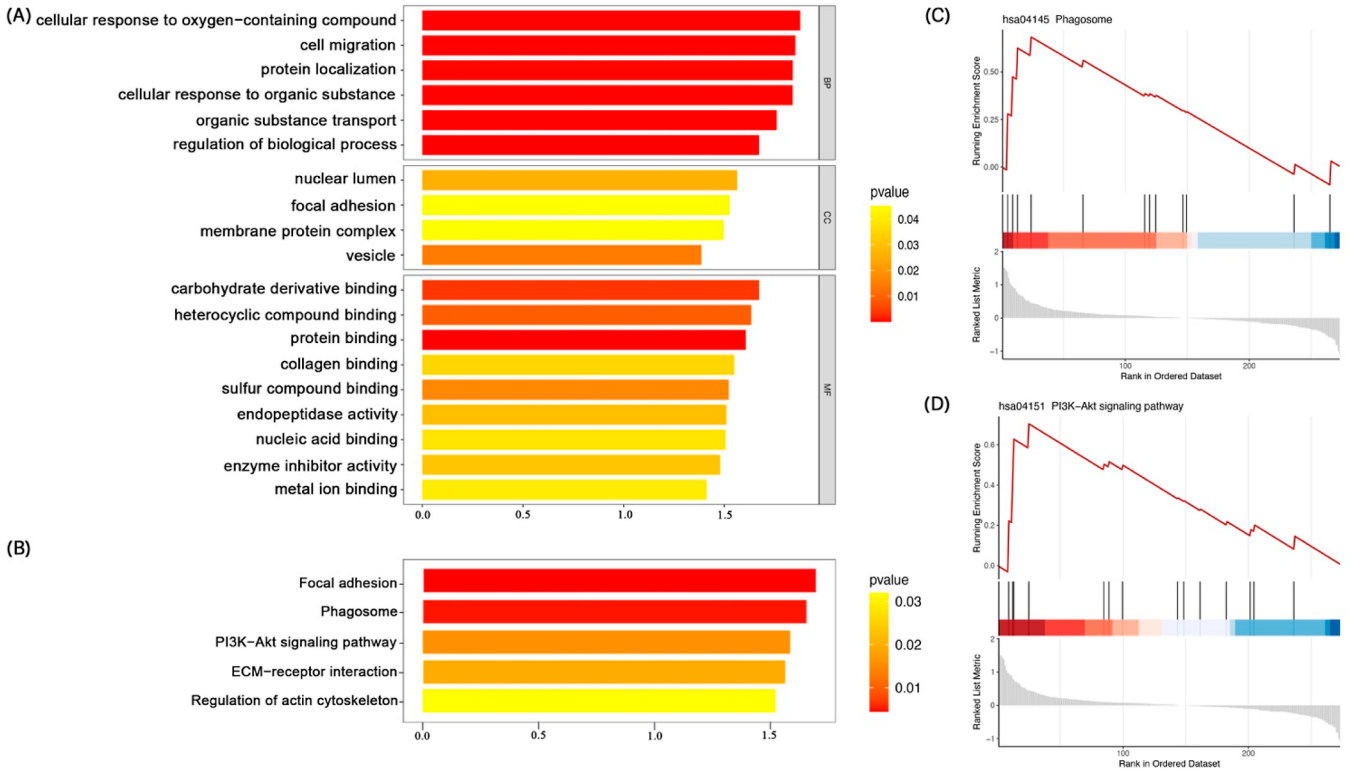

Figure 3. GSEA-GO and GSEA-KEGG analysis. (A) Most significantly enriched GSEA-GO pathways. (B) Most significantly enriched GSEA-KEEG pathways. Each pathway was ranked by normalized enrichment scores (NES). (C,D) GSEA-based KEGG-enrichment plots illustrating representative gene sets, including phagosome and the PI3K-Akt signaling pathway. The red line is indicative of enrichment profile.

ROC Curve Analysis

ROC curve analysis was employed to assess the efficacy of candidate biomarkers (Figure 5A). The findings indicated that the combination of PRSS1 and ACTB, PRSS3, ACTB, PRSS1, and PPBP alone had AUC values above 0.7, while HP, PF4V1, THBS1, and RPL11 had AUC values above 0.6, with sensitivity values predominantly surpassing 50% and specificity values consistently exceeding 80%, and these findings exhibited notable clinical promise. Importantly, the combination of PRSS1 and ACTB yielded enhancements in the AUC, sensitivity, and specificity values. These findings indicated that the combination of PRSS1 and ACTB may function as biomarkers for the early diagnosis of IESS. The plasma levels of PRSS3, ACTB, PRSS1, PPBP, HP, PF4V1, THBS1, and RPL11 in IESS patients were significantly elevated compared with those in healthy controls (Figure 5B).

DISCUSSION

To date, the etiology and pathogenesis of IESS remain largely unresolved. Research studies on lesion tissue from epilepsy patients and animal models have revealed the notable roles of neuroinflammation and oxidative stress pathways in the development and occurrence of epilepsy. Corresponding treatment strategies targeting these mechanisms have been identified.[10,11] Vitchayaporn et al. conducted an analysis of the plasma proteomics of children with refractory epilepsy and identified haptoglobin, interferon-c, and interleukin-1b as promising biomarkers for pediatric refractory epilepsy.[7] Ji Sun et al. conducted a proteomic analysis of children with Rolandic epilepsy and migraine, uncovering potential contributions of immune responses, complement, and fibrinogen systems, as well as glycolytic biological pathways to the genesis of epilepsy.[8] However, the proteomic analysis of the pathogenesis of epilepsy, especially IESS, has rarely been conducted. Employing a bioenrichment pathway approach could enhance the identification of proteins or pathways, providing insights into the potential underlying causes and prognostic mechanisms of IESS. In the present study, a total of 124 DEPs were detected in IESS patients compared with healthy controls through DIA proteomics analysis. Among them, 24 DEPs were identified as the most prominently differentially expressed, exhibiting both up and downregulation, suggesting a potential association with the mechanism of the disorder. This investigation sheds light on the protein profiles in IESS patients' plasma samples.

The present study identified the predominant pathways associated with the DEPs in IESS patients. The GO analysis revealed enrichment in pathways involving cytokines, chemokines, oxidative detoxification, and haptoglobin binding. The KEGG pathway analysis highlighted pathways related to the cytokine−cytokine receptor interaction, the chemokine signaling pathway, and the phagosome. Cytokines and chemokines, key regulators of inflammation, could be implicated in the development of epilepsy.[12−15] These entities can arise from the activation of the microglia, the primary immune cells of the central nervous system,[16] leading to simultaneous induction of diverse inflammatory pathways in the brain.[17] Brain inflammation plays a pivotal role in the pathophysiological mechanisms of various types of epilepsy, including IESS. Oxidative stress, associated with refractory epilepsy, could be triggered by neuroinflammation, yet mitigated by a ketogenic diet through enhanced levels of antioxidants and detoxification enzymes.[18] Moreover, the role of haptoglobin in attenuating neuroinflammation is noteworthy, and plasma haptoglobin was proposed as a potential biomarker for refractory epilepsy.[7,19]

https://doi.org/10.1021/acs.jproteome.4c00298
J. Proteome Res. 2024, 23, 4316−4326

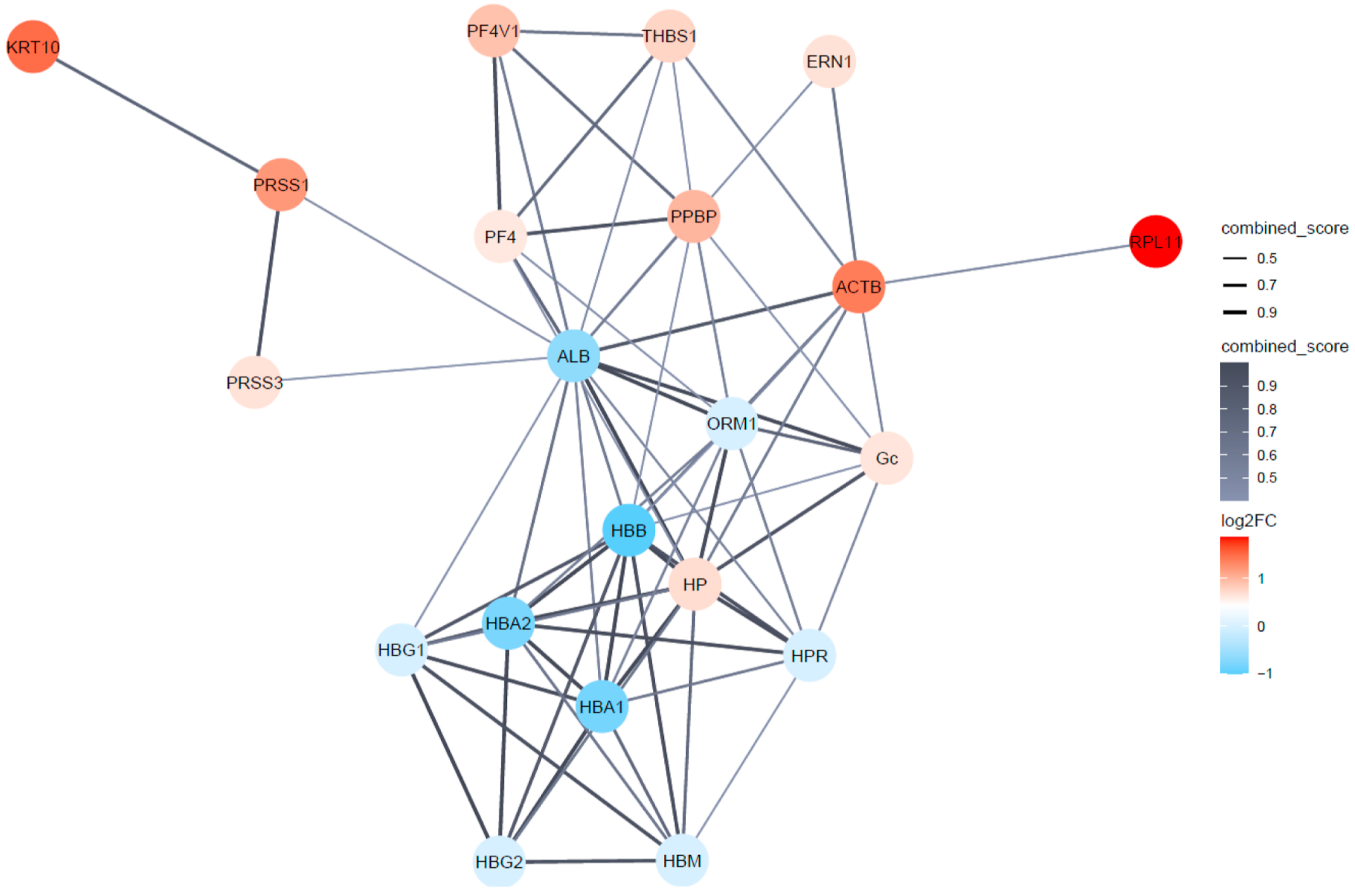

Figure 4. Schematic representation of the PPI network of the DEPs. The line width of the interactions corresponds to the combined interaction score of each interaction, ranging from 0.4 to 1. A wider line indicates a higher score, while a narrower line suggests a lower score. A score of 0.4 represents a medium score, 0.7 indicates a high level, and 0.9 indicates a very high level of interaction confidence. Additionally, different colors were used to denote individual proteins based on their fold change (|log2FC|). The confidence score of interaction is 0.4. In the network, ACTB, PF4V1, THBS1, HP, PF4, and PPBP serve as hub proteins.

Phagocytosis is central to tissue inflammation, autophagy, and immune regulation, significantly contributing to inflammatory responses. The relevance of autophagy mechanisms to the pathophysiology of epileptogenesis has been demonstrated.[20] Phagocytosis plays a crucial role in synaptic pruning, a process of programmed cell elimination for shaping the brain's connectivity during development. Microglia, by engaging in phagocytosis, contribute to the removal of excess synapses, thereby refining and optimizing the brain's connections for proper functioning.[21] Dysregulation of synaptic pruning, whether insufficient or excessive, may be implicated in various neurodevelopmental disorders, including epilepsy.[22] The significant enrichment of these pathways in IESS patients indicates that these pathways and BPs may play a regulatory role in the development of IESS. At present, adrenocorticotropic hormone (ACTH) remains the primary treatment for IESS. Previous studies[23−26] have demonstrated changes in blood or CSF levels of different proinflammatory cytokines in IESS patients treated with ACTH, indicating immunosuppressive and anti-inflammatory effects of ACTH. ACTH likely exerts its therapeutic effects by suppressing the inflammatory pathways in the brain.

Additionally, GSEA-based GO analysis revealed that cell migration and cellular response to oxygen-containing compounds emerged as pivotal pathways, reinforcing the correlation among inflammation, oxidative stress, and IESS. Furthermore, endopeptidase activity, sulfur compound binding, and mental ion binding were enriched in both GO analysis and GSEA-GO analysis. Three pathways may impact the pathogenesis of IESS. Through GSEA-based KEGG pathway analysis, it was found that the phagosome, PI3K-Akt signaling pathway, and focal adhesion were associated with IESS. The phagosome pathway, in conjunction with the aforementioned findings of the KEGG pathway analysis, further substantiated its potential association with IESS. The PI3K-Akt signaling pathway has been implicated in diverse cellular functions, encompassing nutrient uptake, cell proliferation, growth, autophagy, apoptosis, and migration.[27,28] Dysregulation of the pathway has been implicated as a fundamental factor in numerous neurodevelopmental diseases, including epilepsy.[29] Regarding focal adhesions, a great number of components have been identified by proteomics in very large G protein-coupled receptor-1 (VLGR1), which is associated with epilepsy.[30] Hence, the results of GSEA-based GO and KEEG pathway analyses were consistent with the findings of the GO and KEEG pathway analyses in several pathways in this study. These functional analyses of DEPs shed light on the potential underlying pathogenesis of IESS.

In order to establish a robust predictive model for disease diagnosis and explore potential plasma biomarkers, ROC curve analysis was utilized to evaluate the discriminatory ability of DEPs. Notably, PRSS3, ACTB, and PRSS1 exhibited the highest prediction scores. The protein encoded by *ACTB*, known as

https://doi.org/10.1021/acs.jproteome.4c00298
J. Proteome Res. 2024, 23, 4316−4326

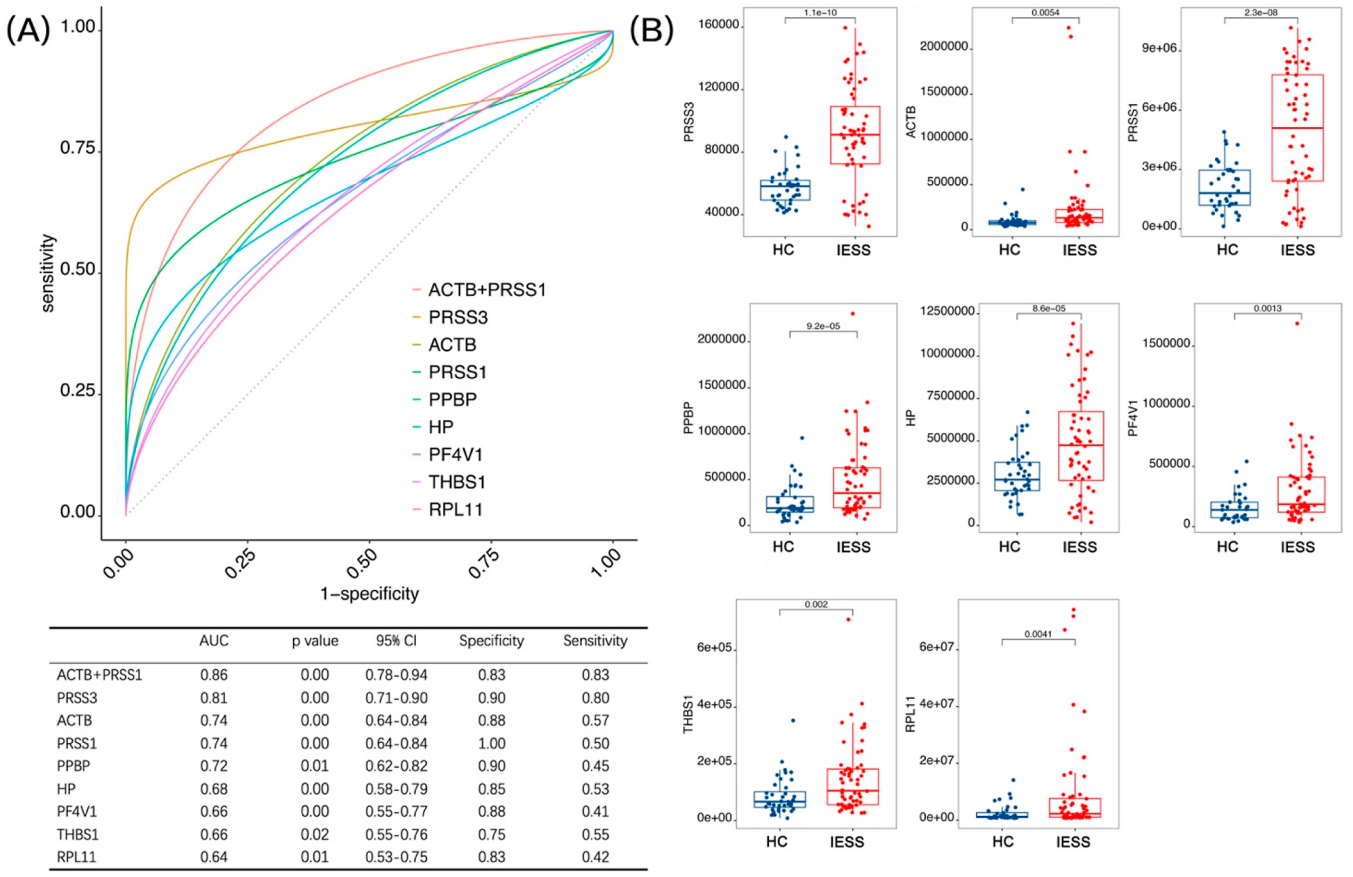

	AUC	p value	95% CI	Specificity	Sensitivity
ACTB+PRSS1	0.86	0.00	0.78-0.94	0.83	0.83
PRSS3	0.81	0.00	0.71-0.90	0.90	0.80
ACTB	0.74	0.00	0.64-0.84	0.88	0.57
PRSS1	0.74	0.00	0.64-0.84	1.00	0.50
PPBP	0.72	0.01	0.62-0.82	0.90	0.45
HP	0.68	0.00	0.58-0.79	0.85	0.53
PF4V1	0.66	0.00	0.55-0.77	0.88	0.41
THBS1	0.66	0.02	0.55-0.76	0.75	0.55
RPL11	0.64	0.01	0.53-0.75	0.83	0.42

Figure 5. Validation and assessment of potential biomarkers. (A) Receiver operating characteristic (ROC) curve analysis of IESS samples versus healthy control samples to validate candidate biomarkers. The models included eight candidate biomarkers and one integrating ACTB + PRSS1. (B) Quantification of plasma levels of PRSS3, ACTB, PRSS1, PPBP, HP, PF4V1, THBS1, and RPL11 in healthy controls and IESS patients. $P < 0.05$ indicates a significant difference in quantification between the two groups.

actin beta, plays crucial roles in cellular processes, including cell motility, cellular morphology maintenance, cell division, and intracellular transportation mechanisms.[31,32] Mutations in this gene have been found to be linked to epilepsy, developmental disorders, and malformations.[33] There is compelling evidence linking neuronal migration disorders with epileptogenesis.[34,35] The upregulation of this protein may contribute to neuronal migration disorders, subsequently leading to IESS. The *PRSS1* encodes serine protease 1, which is essential in fighting against infections, activating blood coagulation or blood clot lysis systems, activating digestive enzymes, and reproduction.[36] Mutations in this gene are associated with autosomal dominant hereditary pancreatitis.[37] Liu et al. identified *PRSS1* as a potential key gene linked to cognitive impairment induced by cadmium exposure in rats,[38] indicating that the *PRSS1* gene may contribute to central nervous system disorders. The *PRSS3* gene encodes both mesotrypsinogen and trypsinogen 4. Prior research demonstrated that trypsin and other trypsin-like serine proteases are instrumental in neural development, plasticity, and neurodegeneration.[39] In the present study, it was hypothesized that PRSS3, ACTB, and PRSS1, as well as the other five proteins verified by ROC curve analysis, could be considered as potential plasma biomarkers for IESS.

The present proteomic discoveries hold promise in offering more precise biomarkers for IESS. Changes in protein levels may precede the structural alterations detectable by brain magnetic resonance imaging (MRI) or aberrant electrical activity observed in EEG, particularly in cases with atypical clinical symptoms. Therefore, proteomic analysis has the potential to promote the early identification of IESS, even prior to manifestations evident through conventional diagnostic modalities. Furthermore, integrating the current proteomic data with established diagnostic methods, such as MRI and EEG, could enhance the accuracy and reliability of diagnosis, forming a more comprehensive diagnostic profile. In cases where genetic testing results are abnormal, proteomic findings may unveil protein irregularities directly related to genetic variants, thereby promoting the identification of disease-associated genes and pathways.[40] Moreover, these findings could advance personalized medicine by identifying protein signatures unique to individual patients,[41] thereby providing tailored treatments based on their specific molecular profiles.

However, the limitations of this study should be pointed out. This study concentrated solely on the examination of the proteome in plasma samples from 60 patients with IESS. The potential diagnostic biomarker was identified based only on the samples included in this study. Moreover, the differential proteins identified in this study were not confirmed by other detection methods. Other analytical techniques are required to confirm the differential proteins found. To advance the identified proteins into a biomarker panel for clinical use, further validation in other models and examination in a larger population would be necessary.

https://doi.org/10.1021/acs.jproteome.4c00298
J. Proteome Res. 2024, 23, 4316−4326

CONCLUSIONS

In conclusion, this study identified 124 DEPs that were potentially associated with the pathogenesis of IESS through DIA proteomics analysis of blood samples obtained from IESS patients and healthy controls. The involvement of inflammation, cytokines, chemokines, oxidative detoxification, phagosomes, and other related pathways indicated their potential roles in the occurrence and development of IESS. Considering the availability of serine protease 1-related detection kits on the market, simultaneous detection of β-actin and serine protease 1 may provide novel insights for the identification of potential plasma biomarkers for diagnosing IESS. The findings highlighted potential biomarker candidates for identifying IESS patients while suggesting therapeutic targets for customized treatment approaches.

ASSOCIATED CONTENT

Data Availability Statement

The raw data for this study can be accessed via ProteomeXchange (Identifier: PXD052465).

Supporting Information

The Supporting Information is available free of charge at https://pubs.acs.org/doi/10.1021/acs.jproteome.4c00298.

PCA of all samples; each bubble representing one sample, with green bubbles representing IESS patients and blue bubbles representing healthy controls; degree of aggregation reflects the similarity in protein expression profiles among the samples; and Venn diagram illustrating the number of proteins that are common and unique to IESS patients and healthy controls (PDF)

Details of 124 DEPs; details of the GO analysis; details of the KEGG analysis; details of the GSEA-GO analysis; and details of the GSEA-KEEG analysis (XLSX)

AUTHOR INFORMATION

Corresponding Author

Dongfang Zou − *Epilepsy Center and Department of Neurology, Shenzhen Children's Hospital, Shenzhen 518000 Guangdong, China;* orcid.org/0000-0001-6726-8704; Phone: +86-18938690738; Email: fiesta_zou@163.com

Authors

Haohua Huang − *Epilepsy Center and Department of Neurology, Shenzhen Children's Hospital, Shenzhen 518000 Guangdong, China; Shenzhen Pediatrics Institute of Shantou University Medical College, Shenzhen 518000 Guangdong, China*

Dezhi Cao − *Epilepsy Center and Department of Neurology, Shenzhen Children's Hospital, Shenzhen 518000 Guangdong, China*

Yan Hu − *Epilepsy Center and Department of Neurology, Shenzhen Children's Hospital, Shenzhen 518000 Guangdong, China*

Qianqian He − *Epilepsy Center and Department of Neurology, Shenzhen Children's Hospital, Shenzhen 518000 Guangdong, China*

Xia Zhao − *Epilepsy Center and Department of Neurology, Shenzhen Children's Hospital, Shenzhen 518000 Guangdong, China*

Li Chen − *Epilepsy Center and Department of Neurology, Shenzhen Children's Hospital, Shenzhen 518000 Guangdong, China*

Sufang Lin − *Epilepsy Center and Department of Neurology, Shenzhen Children's Hospital, Shenzhen 518000 Guangdong, China*

Xufeng Luo − *Epilepsy Center and Department of Neurology, Shenzhen Children's Hospital, Shenzhen 518000 Guangdong, China*

Yuanzhen Ye − *Epilepsy Center and Department of Neurology, Shenzhen Children's Hospital, Shenzhen 518000 Guangdong, China*

Jianxiang Liao − *Epilepsy Center and Department of Neurology, Shenzhen Children's Hospital, Shenzhen 518000 Guangdong, China*

Huafang Zou − *Epilepsy Center and Department of Neurology, Shenzhen Children's Hospital, Shenzhen 518000 Guangdong, China*

Complete contact information is available at: https://pubs.acs.org/10.1021/acs.jproteome.4c00298

Author Contributions

H.H., D.C., and Y.H. contributed equally to the manuscript. D.Z. designed the study, administered the project, analyzed the data, and revised the manuscript. H.H. and Q.H. completed the collection of the clinical data. H.H. assisted analysis of the data and completed the draft of the manuscript. D.C. and Y.H. completed the recruitment of the patients and contributed to clinical data interpretation. X.Z., L.C., S.L., X.L., and Y.Y. performed data analysis and provided technical assistance. J.L. and H.Z. contributed to data analysis and interpretation. All authors have read and approved the final manuscript.

Funding

This study was supported by grants from the Shenzhen Science and Technology Program (grant no. JCYJ20210324135010029), the Sanming Project of Medicine in Shenzhen (grant no. SZSM202311028), the Shenzhen Key Medical Discipline Construction Fund (grant no. SZXK033), and the Shenzhen Fund for Guangdong Provincial High-level Clinical Key Specialties (grant no. SZGSP012).

Notes

The authors declare no competing financial interest.

ACKNOWLEDGMENTS

We express our gratitude to Medjaden Inc. for providing scientific editing services for this manuscript.

REFERENCES

(1) Zuberi, S. M.; Wirrell, E.; Yozawitz, E.; Wilmshurst, J. M.; Specchio, N.; Riney, K.; Pressler, R.; Auvin, S.; Samia, P.; Hirsch, E.; Galicchio, S.; Triki, C.; Snead, O. C.; Wiebe, S.; Cross, J. H.; Tinuper, P.; Scheffer, I. E.; Perucca, E.; Moshé, S. L.; Nabbout, R. ILAE classification and definition of epilepsy syndromes with onset in neonates and infants: Position statement by the ILAE Task Force on Nosology and Definitions. *Epilepsia* **2022**, *63* (6), 1349−1397.

(2) Mackay, M. T.; Weiss, S. K.; Adams-Webber, T.; Ashwal, S.; Stephens, D.; Ballaban-Gill, K.; Baram, T. Z.; Duchowny, M.; Hirtz, D.; Pellock, J. M.; Shields, W. D.; Shinnar, S.; Wyllie, E.; Snead, O. C. Practice parameter: medical treatment of infantile spasms: report of the American Academy of Neurology and the Child Neurology Society. *Neurology* **2004**, *62* (10), 1668−1681.

(3) Kelley, S. A.; Knupp, K. G. Infantile Spasms-Have We Made Progress? *Curr. Neurol. Neurosci. Rep.* **2018**, *18* (5), 27.
(4) Berg, A. T.; Berkovic, S. F.; Brodie, M. J.; Buchhalter, J.; Cross, J. H.; van Emde Boas, W.; Engel, J.; French, J.; Glauser, T. A.; Mathern, G. W.; Moshé, S. L.; Nordli, D.; Plouin, P.; Scheffer, I. E. Revised terminology and concepts for organization of seizures and epilepsies: report of the ILAE Commission on Classification and Terminology, 2005−2009. *Epilepsia* **2010**, *51* (4), 676−685.
(5) Khan, S.; Al Baradie, R. Epileptic encephalopathies: an overview. *Epilepsy Res. Treat.* **2012**, *2012*, 1−8.
(6) Riikonen, R. S. Favourable prognostic factors with infantile spasms. *Eur. J. Paediatr. Neurol.* **2010**, *14* (1), 13−18.
(7) Saengow, V. E.; Chiangjong, W.; Khongkhatithum, C.; Changtong, C.; Chokchaichamnankit, D.; Weeraphan, C.; Kaewboonruang, P.; Thampratankul, L.; Manuyakorn, W.; Hongeng, S.; Srisomsap, C.; Svasti, J.; Chutipongtanate, S.; Visudtibhan, A. Proteomic analysis reveals plasma haptoglobin, interferon-γ, and interleukin-1β as potential biomarkers of pediatric refractory epilepsy. *Brain Dev.* **2021**, *43* (3), 431−439.
(8) Sun, J.; Jiang, T.; Gu, F.; Ma, D.; Liang, J. TMT-Based Proteomic Analysis of Plasma from Children with Rolandic Epilepsy. *Dis. Markers* **2020**, *2020*, 1−10.
(9) Szklarczyk, D.; Gable, A. L.; Lyon, D.; Junge, A.; Wyder, S.; Huerta-Cepas, J.; Simonovic, M.; Doncheva, N. T.; Morris, J. H.; Bork, P.; Jensen, L. J.; Mering, C. V. STRING v11: protein-protein association networks with increased coverage, supporting functional discovery in genome-wide experimental datasets. *Nucleic Acids Res.* **2019**, *47* (D1), D607−d613.
(10) Devinsky, O.; Vezzani, A.; O'Brien, T. J.; Jette, N.; Scheffer, I. E.; de Curtis, M.; Perucca, P. Epilepsy. *Nat. Rev. Dis. Primers* **2018**, *4*, 18024.
(11) Klein, P.; Dingledine, R.; Aronica, E.; Bernard, C.; Blümcke, I.; Boison, D.; Brodie, M. J.; Brooks-Kayal, A. R.; Engel, J., Jr; Forcelli, P. A.; Hirsch, L. J.; Kaminski, R. M.; Klitgaard, H.; Kobow, K.; Lowenstein, D. H.; Pearl, P. L.; Pitkänen, A.; Puhakka, N.; Rogawski, M. A.; Schmidt, D.; Sillanpää, M.; Sloviter, R. S.; Steinhäuser, C.; Vezzani, A.; Walker, M. C.; Löscher, W. Commonalities in epileptogenic processes from different acute brain insults: Do they translate? *Epilepsia* **2018**, *59* (1), 37−66.
(12) Turner, M. D.; Nedjai, B.; Hurst, T.; Pennington, D. J. Cytokines and chemokines: At the crossroads of cell signalling and inflammatory disease. *Biochim. Biophys. Acta* **2014**, *1843* (11), 2563−2582.
(13) Barker-Haliski, M. L.; Löscher, W.; White, H. S.; Galanopoulou, A. S. Neuroinflammation in epileptogenesis: Insights and translational perspectives from new models of epilepsy. *Epilepsia* **2017**, *58* (S3), 39−47.
(14) Jaseja, H. A plausible explanation for superiority of adreno-cortico-trophic hormone (ACTH) over oral corticosteroids in management of infantile spasms (West syndrome). *Med. Hypotheses* **2006**, *67* (4), 721−724.
(15) Vezzani, A.; Balosso, S.; Ravizza, T. Neuroinflammatory pathways as treatment targets and biomarkers in epilepsy. *Nat. Rev. Neurol.* **2019**, *15* (8), 459−472.
(16) Scheiblich, H.; Trombly, M.; Ramirez, A.; Heneka, M. T. Neuroimmune Connections in Aging and Neurodegenerative Diseases. *Trends Immunol.* **2020**, *41* (4), 300−312.
(17) Vezzani, A.; Aronica, E.; Mazarati, A.; Pittman, Q. J. Epilepsy and brain inflammation. *Exp. Neurol.* **2013**, *244*, 11−21.
(18) Milder, J.; Patel, M. Modulation of oxidative stress and mitochondrial function by the ketogenic diet. *Epilepsy Res.* **2012**, *100* (3), 295−303.
(19) Tan, H.; Bi, J.; Wang, Y.; Zhang, J.; Zuo, Z. Transfusion of Old RBCs Induces Neuroinflammation and Cognitive Impairment. *Crit. Care Med.* **2015**, *43* (8), e276−e286.
(20) Zhu, H.; Wang, W.; Li, Y. Molecular Mechanism and Regulation of Autophagy and Its Potential Role in Epilepsy. *Cells* **2022**, *11* (17), 2621.
(21) Li, X.; Li, Y.; Jin, Y.; Zhang, Y.; Wu, J.; Xu, Z.; Huang, Y.; Cai, L.; Gao, S.; Liu, T.; Zeng, F.; Wang, Y.; Wang, W.; Yuan, T. F.; Tian, H.; Shu, Y.; Guo, F.; Lu, W.; Mao, Y.; Mei, X.; Rao, Y.; Peng, B. Transcriptional and epigenetic decoding of the microglial aging process. *Nat. Aging* **2023**, *3* (10), 1288−1311.
(22) Neniskyte, U.; Gross, C. T. Errant gardeners: glial-cell-dependent synaptic pruning and neurodevelopmental disorders. *Nat. Rev. Neurosci.* **2017**, *18* (11), 658−670.
(23) Vezzani, A.; French, J.; Bartfai, T.; Baram, T. Z. The role of inflammation in epilepsy. *Nat. Rev. Neurol.* **2011**, *7* (1), 31−40.
(24) Haginoya, K.; Noguchi, R.; Zhao, Y.; Munakata, M.; Yokoyama, H.; Tanaka, S.; Hino-Fukuyo, N.; Uematsu, M.; Yamamoto, K.; Takayanagi, M.; Iinuma, K.; Tsuchiya, S. Reduced levels of interleukin-1 receptor antagonist in the cerebrospinal fluid in patients with West syndrome. *Epilepsy Res.* **2009**, *85* (2−3), 314−317.
(25) Türe, E.; Kamaşak, T.; Cora, M.; Şahin, S.; Arslan, E. A.; Kaklıkaya, N.; Cansu, A. Comparison of the serum cytokine levels before and after adrenocorticotropic hormone (ACTH) therapy in patients with infantile spasm. *Seizure* **2016**, *41*, 112−115.
(26) Yamanaka, G.; Morishita, N.; Morichi, S.; Takeshita, M.; Tomomi, U.; Ishida, Y.; Tomoko, T.; Oana, S.; Watanabe, Y.; Go, S.; Kashiwagi, Y.; Kawashima, H. Serial Analysis of Multiple Serum Cytokine Responses to Adrenocorticotropic Hormone Therapy in Patients With West Syndrome. *J. Child Neurol.* **2018**, *33* (8), 528−533.
(27) Hennessy, B. T.; Smith, D. L.; Ram, P. T.; Lu, Y.; Mills, G. B. Exploiting the PI3K/AKT pathway for cancer drug discovery. *Nat. Rev. Drug Discov.* **2005**, *4* (12), 988−1004.
(28) Yu, J. S.; Cui, W. Proliferation, survival and metabolism: the role of PI3K/AKT/mTOR signalling in pluripotency and cell fate determination. *Development* **2016**, *143* (17), 3050−3060.
(29) Wang, L.; Zhou, K.; Fu, Z.; Yu, D.; Huang, H.; Zang, X.; Mo, X. Brain Development and Akt Signaling: the Crossroads of Signaling Pathway and Neurodevelopmental Diseases. *J. Mol. Neurosci.* **2017**, *61* (3), 379−384.
(30) Kusuluri, D. K.; Güler, B. E.; Knapp, B.; Horn, N.; Boldt, K.; Ueffing, M.; Aust, G.; Wolfrum, U. Adhesion G protein-coupled receptor VLGR1/ADGRV1 regulates cell spreading and migration by mechanosensing at focal adhesions. *iScience* **2021**, *24* (4), 102283.
(31) Sheterline, P.; Clayton, J.; Sparrow, J. Actin. *Protein Profile* **1995**, *2* (1), 1−103.
(32) Tondeleir, D.; Vandamme, D.; Vandekerckhove, J.; Ampe, C.; Lambrechts, A. Actin isoform expression patterns during mammalian development and in pathology: insights from mouse models. *Cell Motil. Cytoskeleton* **2009**, *66* (10), 798−815.
(33) Rivière, J. B.; van Bon, B. W.; Hoischen, A.; Kholmanskikh, S. S.; O'Roak, B. J.; Gilissen, C.; Gijsen, S.; Sullivan, C. T.; Christian, S. L.; Abdul-Rahman, O. A.; Atkin, J. F.; Chassaing, N.; Drouin-Garraud, V.; Fry, A. E.; Fryns, J. P.; Gripp, K. W.; Kempers, M.; Kleefstra, T.; Mancini, G. M.; Nowaczyk, M. J.; van Ravenswaaij-Arts, C. M.; Roscioli, T.; Marble, M.; Rosenfeld, J. A.; Siu, V. M.; de Vries, B. B.; Shendure, J.; Verloes, A.; Veltman, J. A.; Brunner, H. G.; Ross, M. E.; Pilz, D. T.; Dobyns, W. B. De novo mutations in the actin genes ACTB and ACTG1 cause Baraitser-Winter syndrome. *Nat. Genet.* **2012**, *44* (4), 440−444. s441−442
(34) Guerrini, R.; Filippi, T. Topical Review: Neuronal Migration Disorders, Genetics, and Epileptogenesis. *J. Child Neurol.* **2005**, *20* (4), 287−299.
(35) Liu, J. S. Molecular genetics of neuronal migration disorders. *Curr. Neurol. Neurosci. Rep.* **2011**, *11* (2), 171−178.
(36) Chan, E. D.; King, P. T.; Bai, X.; Schoffstall, A. M.; Sandhaus, R. A.; Buckle, A. M. The Inhibition of Serine Proteases by Serpins Is Augmented by Negatively Charged Heparin: A Concise Review of Some Clinically Relevant Interactions. *Int. J. Mol. Sci.* **2024**, *25* (3), 1804.
(37) Zou, W. B.; Cooper, D. N.; Masson, E.; Pu, N.; Liao, Z.; Férec, C.; Chen, J. M. Trypsinogen (PRSS1 and PRSS2) gene dosage correlates with pancreatitis risk across genetic and transgenic studies: a systematic review and re-analysis. *Hum. Genet.* **2022**, *141* (8), 1327−1338.
(38) Liu, H.; Wan, X.; Yao, L.; Zhao, Q.; Yang, Y.; Liu, H.; Shang, J.; Zeng, F.; Wang, X.; Huang, S. Differentially expressed long non-coding

https://doi.org/10.1021/acs.jproteome.4c00298
J. Proteome Res. 2024, 23, 4316−4326

RNAs and mRNAs of cadmium exposure on learning disability of offspring rats. *Eur. J. Med. Res.* **2024**, *29* (1), 82.
(39) Koistinen, H.; Koistinen, R.; Zhang, W. M.; Valmu, L.; Stenman, U. H. Nexin-1 inhibits the activity of human brain trypsin. *Neuroscience* **2009**, *160* (1), 97−102.
(40) Ferkingstad, E.; Sulem, P.; Atlason, B. A.; Sveinbjornsson, G.; Magnusson, M. I.; Styrmisdottir, E. L.; Gunnarsdottir, K.; Helgason, A.; Oddsson, A.; Halldorsson, B. V.; Jensson, B. O.; Zink, F.; Halldorsson, G. H.; Masson, G.; Arnadottir, G. A.; Katrinardottir, H.; Juliusson, K.; Magnusson, M. K.; Magnusson, O. T.; Fridriksdottir, R.; Saevarsdottir, S.; Gudjonsson, S. A.; Stacey, S. N.; Rognvaldsson, S.; Eiriksdottir, T.; Olafsdottir, T. A.; Steinthorsdottir, V.; Tragante, V.; Ulfarsson, M. O.; Stefansson, H.; Jonsdottir, I.; Holm, H.; Rafnar, T.; Melsted, P.; Saemundsdottir, J.; Norddahl, G. L.; Lund, S. H.; Gudbjartsson, D. F.; Thorsteinsdottir, U.; Stefansson, K. Large-scale integration of the plasma proteome with genetics and disease. *Nat. Genet.* **2021**, *53* (12), 1712−1721.
(41) Striano, P.; Minassian, B. A. From Genetic Testing to Precision Medicine in Epilepsy. *Neurotherapeutics* **2020**, *17* (2), 609−615.

https://doi.org/10.1021/acs.jproteome.4c00298
J. Proteome Res. 2024, 23, 4316−4326